British Journal of Cancer www.nature.com/bjc

ARTICLE

Translational Therapeutics

CXCR1/2 dual-inhibitor ladarixin reduces tumour burden and promotes immunotherapy response in pancreatic cancer

Geny Piro[1,8], Carmine Carbone[1,8], Antonio Agostini[1], Annachiara Esposito[1], Maria De Pizzol[2], Rubina Novelli[2], Marcello Allegretti[2], Andrea Aramini[2], Alessia Caggiano[1], Alessia Granitto[3], Francesco De Sanctis[4], Stefano Ugel[4], Vincenzo Corbo[5,6], Maurizio Martini[3], Rita Teresa Lawlor[5,6], Aldo Scarpa[5,6] and Giampaolo Tortora[1,7]✉

BACKGROUND: Pancreatic ductal adenocarcinoma (PDAC) is a highly lethal malignancy with few therapeutic options available. Despite immunotherapy has revolutionised cancer treatment, the results obtained in PDAC are still disappointing. Emerging evidence suggests that chemokines/CXCRs-axis plays a pivotal role in immune tumour microenvironment modulation, which may influence immunotherapy responsiveness. Here, we evaluated the effectiveness of CXCR1/2 inhibitor ladarixin, alone or in combination with anti-PD-1, against immunosuppression in PDAC.

METHODS: A set of preclinical models was obtained by engrafting mouse PDAC-derived cells into syngeneic immune-competent mice, as well as by orthotopically transplanting patient-derived PDAC tumour into human immune-system-reconstituted (HIR) mice (HuCD34-NSG-mice). Tumour-bearing mice were randomly assigned to receive vehicles, ladarixin, anti-PD-1 or drugs combination.

RESULTS: CXCR1/2 inhibition by ladarixin reverted in vitro tumour-mediated M2 macrophages polarisation and migration. Ladarixin as single agent reduced tumour burden in cancer-derived graft (CDG) models with high-immunogenic potential and increased the efficacy of ICI in non-immunogenic CDG-resistant models. In a HIR mouse model bearing the immunogenic subtype of human PDAC, ladarixin showed high efficacy increasing the antitumor effect of anti-PD-1.

CONCLUSION: Ladarixin in combination with anti-PD-1 might represent an extremely effective approach for the treatment of immunotherapy refractory PDAC, allowing pro-tumoral to immune-permissive microenvironment conversion.

British Journal of Cancer (2023) 128:331–341; https://doi.org/10.1038/s41416-022-02028-6

INTRODUCTION

Pancreatic ductal adenocarcinoma (PDAC) is one of the most aggressive and lethal malignancies for which no effective pharmacological treatments are currently available. For most PDAC patients, the prognosis is extremely poor because of the advanced stage at diagnosis and the scarce response to conventional chemotherapy and radiotherapy [1]. Unfortunately, also novel immunotherapies targeting the immune checkpoints T-lymphocyte-associated protein 4 (CTLA-4) and programmed cell death protein 1 (PD-1) have failed so far to show meaningful clinical benefit in unselected patients with PDAC [2–4], and this is primarily due to the fact that PDAC is characterised by an immunosuppressive tumour microenvironment (TME) that can hinder immunotherapy effects [5].

Although PDAC is generally considered an immune "cold" cancer, different PDAC tumour subtypes have diverse immune TME that might differentially influence immunotherapy responsiveness and thus patient survival [6, 7]. Key factors in determining the immunogenicity of PDAC subtypes, and thus their response to immunotherapy, are macrophages recruited to the tumour to become tumour-associated macrophages (TAMs). In response to specific factors in the TME, TAMs can rapidly switch between antitumor (M1) or immunotolerant (M2) phenotype. PDAC subtypes characterised by higher levels of M1 TAMs show a more positive response to immunotherapy with longer overall survival, whereas subtypes with higher levels of M2 TAMs display reduced immunotherapy response and a shorter survival [8].

CXCL8 (IL-8) is one of the primary chemotactic factors that regulates the biology and functions of neutrophils acting through its primary receptors CXCR1 and CXCR2 on their surface [9]. In tumours, IL-8 and its receptors CXCR1-2 have been shown to foster progression through different mechanisms, including impairing antitumor immunity by recruiting myeloid-derived suppressor cells and neutrophils to the TME [10, 11]. Moreover, level of circulating IL-8 has been linked to immunotherapy response [12–16]. Therapeutic blockade of CXCR1 and CXCR2 in

[1]Medical Oncology, Department of Medical and Surgical Sciences Fondazione Policlinico Universitario "Agostino Gemelli" IRCCS, Rome, Italy. [2]Dompé Farmaceutici S.p.A., Via Santa Lucia 6, Milan, Italy. [3]Division of Anatomic Pathology and Histology, Fondazione Policlinico Universitario "Agostino Gemelli" IRCCS, Rome, Italy. [4]Department of Medicine, Section of Immunology, University of Verona, Verona, Italy. [5]Department of Diagnostics and Public Health, Section of Pathology, University and Hospital Trust of Verona, Verona, Italy. [6]ARC-Net Research Centre, University and Hospital Trust of Verona, Verona, Italy. [7]Medical Oncology, Department of Translational Medicine, Catholic University of the Sacred Heart, Rome, Italy. [8]These authors jointly supervised this work: Geny Piro, Carmine Carbone. ✉email: giampaolo.tortora@policlinicogemelli.it

Received: 19 May 2022 Revised: 11 October 2022 Accepted: 13 October 2022
Published online: 16 November 2022

tumour preclinical models has been shown to favour anticancer immune responses by inhibiting recruitment and accumulation of immunosuppressive tumour-associated neutrophils (TANs) [11, 17].

While the effects of IL-8 and its inhibition on TANs have been widely investigated, little is still known about the effects that IL-8/CXCR1-2 axis inhibition can have on TAMs and, especially, on how these effects might potentially affect PDAC pathology and treatment. Here, we evaluated the effectiveness of a dual CXCR1/CXCR2 inhibitor (ladarixin), given alone or in combination with anti-PD-1, against immunosuppression in immunocompetent PDAC mouse models with distinct degrees of immune coldness, focusing on its effects on macrophage recruitment and polarisation. As crucial limitations have emerged studying the biology of the IL-8/CXCR pathway in murine animal models [18], we then also evaluated the effects of the different treatments in a patient-derived xenograft (PDX) model from a PDAC patient sample transplanted in human immune-reconstituted (HIR) mice. Indeed, humanised mouse models have proved to be a key tool to study immunotherapy response [19–21].

METHODS

Cell lines and materials

Cell lines were kindly provided by Dr. D. Tuveson's lab, at Cold Spring Harbor Laboratory (New York, USA) and Dr. P. Cappello's lab, at CeRMS laboratory (Turin, Italy), and were maintained in their original culturing conditions [22–24]. hi cells were daily checked by morphology and routinely tested to be mycoplasma free by PCR assay. Ladarixin was provided by Dompè Farmaceutici spa (Milano, Italy). Murine anti-PD-1 and the relative control were purchased from Leinco Tech (Fento, MO, USA). Nivolumab was from Bristol–Myers Squibb.

Cell proliferation

In total, 1.0×10^3 cells/well were seeded in 96-well plates. At the indicated hours, sulforhodamine B (SRB) (Sigma-Aldrich, St. Louis, Missouri, USA) assay was used to obtain relative estimates of viable cell number according to manufacturer instructions.

RNA isolation and quantitative RT-PCR assay

RNA was obtained using TRizol reagent (Invitrogen Corporation, Carlsbad, California, USA) according to the manufacturer's instructions. The cDNA was evaluated for real-time PCR with QuantStudio 3 (Thermo Fisher Scientific, Waltham, Massachusetts, USA) using a specific primer and SYBR Green. QuantiTect Primer Assays (Qiagen, Hilden, Germany) were used to quantify mouse cDNA levels of Arg1, CD80, CD86, CXCR1 and CXCR2. Gene expression was calculated using $2^{-\mathrm{DDCT}}$ method and normalised to β-actin expression.

Bone marrow-derived macrophage isolation, migration and attraction assays

Bone marrow-derived macrophages (BMDMs) were differentiated in vitro as previously described [25]. Briefly, bone marrow precursors were flushed from long bones of C57BL6 mice and cultured in RPMI supplemented with 10% heat-inactivated-FBS, in the presence of 100 ng/ml of mM-CSF (Miltenyi, Bergisch Gladbach, NRW, Germany) for 7 days with medium change after 4 days. At day 7, adherent cells were cultured with conditioned medium from tumour cells or with complete media containing specific cytokines for macrophages polarisation as control (M1: 100 ng/ml LPS; M2: 10 ng/ml mIL-4, 10 ng/ml mIL-13) (Miltenyi, Bergisch Gladbach, NRW, Germany). At day 10, cells were harvested and analysed for qRT-PCR.

Migration of macrophages was evaluated by wound-healing assay. Macrophages were scratched, washed gently with cold PBS 1X, cultured with conditioned medium from the indicated cancer cell lines and treated or not with ladarixin (10 μM). Photographs of at least five different points were taken using phase contrast microscopy immediately and after the indicated time. The attraction of macrophages by cancer cells was evaluated by using 2 well silicone inserts (Ibidi, Gräfelfing, Germany) with a defined cell-free gap to create co-culture of tumour cells and macrophages that shared medium. Co-cultures were treated or not with ladarixin (10 μM), and attraction of macrophages was assessed after the indicated time.

Syngeneic PDAC mouse models

To generate syngeneic orthotopic PDAC cancer-derived graft (CDG) mouse models, female recipient C57BL6/J mice (4–6 weeks old) were injected with murine pancreatic cancer cell derived from KPC (LSL-Kras G12D/+; Trp53fl/+; Pdx1-Cre) and KC (LSL-Kras G12D/+; Pdx1-Cre) engineered mice that spontaneously develop PDAC. The injection of pancreatic cancer cells was performed as previously described [26, 27]. Cancer cells were resuspended in 1:1 dilution of Matrigel and cold PBS and were subcutaneously injected on the animal flank. The injection was considered successful by the development of bubble without signs of leakage. Following weekly manual palpation starting 10 days following transplantation, tumour-bearing mice were measured by a calliper.

Tumour-bearing mice received Ladarixin (15 mg/kg, i.p. daily for 2 weeks), anti-PD-1 (6 mg/Kg or IgG, i.p. twice a week for 2 weeks) as single agents or in combination settings. Ladarixin dosage was chosen based on previous studies that described pharmacokinetics, pharmacodynamics and pharmacological characterisation of this compound [28, 29].

PBS ang IgG (15 mg/kg, i.p. daily for 2 weeks) were used as control. No significant body weight differences were detected upon treatments. The methods for animal study followed the ARRIVE guidelines 2.0 [30].

Orthotopic human immune-system reconstituted (HIR) patient-derived xenograft (PDX) mouse model

To establish the HIR-PDX model, we selected an immunogenic subtype tumour (according to Bailey et al. classification) [31] from ARCNET Tissue Biobank (University of Verona) showing a compatible HLA with HIR mouse models (HuCD34-NSG^{TM}) (Jackson Laboratory, USA). We matched PDAC patient and CD34 donor according to HLA-DR allele, which contributes most to graft survival in organ transplantation [32]. HIR-PDX mice were obtained through a two-steps process: (1) increase of patient tumour in SCID mice, and (2) implantation of tumour in CD34 Human Immune Reconstituted (HIR) NSG mice" (huNSG-mice).

Briefly, to increase pancreatic cancer tissue, tumour from the patient was reduced into small pieces (2–3 mm) and implanted s.c. in the flanks of immunodeficient (SCID) mice ($n = 3$) (Taconic, Germantown, NY) and propagated by serial transplantation. Mice were monitored for health (body weight) and tumour growth. Mice were euthanized, and subcutaneous tumours were aseptically harvested when a volume of 1000 mm^3 was reached, according to Institutional Animal Care and Use Committee guidelines. A subsequent new generation of xenograft models (PDX) were obtained by orthotopic implantation of tumour cells in the pancreas of "CD34 Human Immune Reconstituted NSG mice" (huNSG-mice) to obtain the HIR-PDX mice ($n = 20$). Briefly, an incision was made in the left abdominal side at the level of the spleen. Cancer cells were resuspended in 1:1 dilution of Matrigel and cold PBS and were injected into the tail region of the pancreas using insulin syringes (25 Gauge). The injection was considered successful by the development of bubble without signs of leakage. The peritoneum was sutured with short-term absorbable suture (Vetsuture), and the skin was closed with wound clips. Mice were randomly assigned to different treatment groups. Following weekly manual palpation starting 10 days following transplantation, tumour-bearing mice were subjected to high-contrast ultrasound screening once a week using the Vevo 2100 System with a MS250, 13–24 MHz scanhead (Visual Sonics, Inc, Amsterdam, NL). In order to determine the early response to treatments, after eleven weeks, a HIR-PDX mouse of each group ($n = 5$) was euthanized by carbon dioxide inhalation. Tumour tissue of each mouse was collected for molecular characterisation by IHC analysis. All treatment groups of HIR-PDX mice were monitored for tumour growth to determine treatments responses. At reaching of cut-off, mice were euthanized, and abdominal cavity opened for direct visualisation of tumours. Tumour tissue of each mouse was collected for IHC as described above. The mice were euthanized using carbon dioxide inhalation when evidence of advanced bulky disease or ascitic abdominal swelling developed, and this was considered the day of death for the purpose of survival evaluation.

Immunohistochemistry and haematoxylin–eosin (H&E) staining

Tissue sections were subjected to H&E, and immunohistochemical staining. A pathologist, who was blinded to treatment allocation of the mice, reviewed the H&E-stained slides of cancer tissues. The following antibodies were used for immunohistochemical staining with established procedures: for murine tissue IHC analysis: CD3 (ab56313), CD11b (ab133357), granzyme (ab53097), CD8 (ab217344), CD68 (ab283654); for human tissue

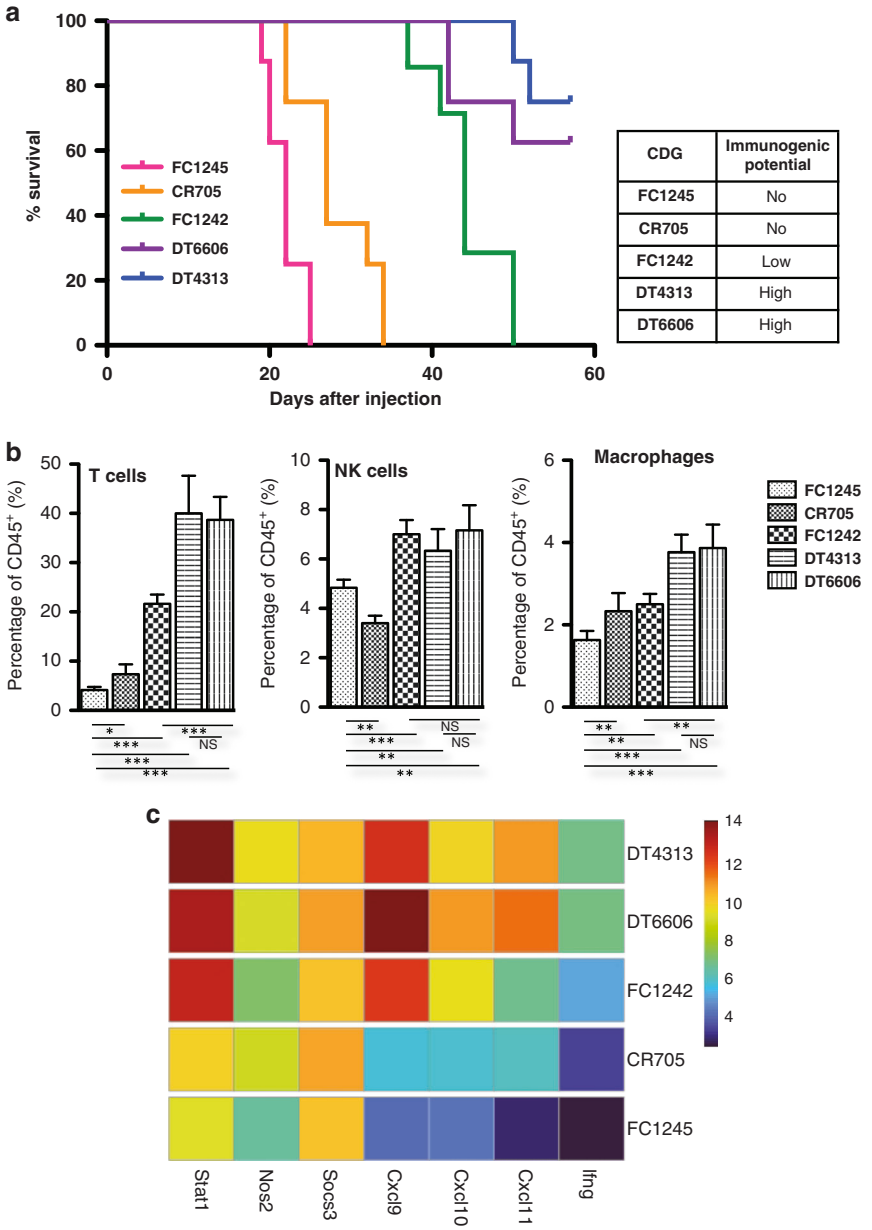

CDG	Immunogenic potential
FC1245	No
CR705	No
FC1242	Low
DT4313	High
DT6606	High

Fig. 1 Orthotopic pancreatic cancer isograft mouse models characterisation. a Kaplan–Meier survival analysis of C57BL/6J mice bearing the indicated pancreatic cancer tumours with different immunologic potential; **b** flow cytometry analysis of immune infiltrating components of tumours from CDG mouse models, T cells (CD45+ CD3 +); Macrophages (CD45, CD11b, f4/80); NK cells (CD45+ CD49b +). The mean values and SD are shown. ***$P < 0.001$, **$P < 0.01$; *$P < 0.05$, by two-tailed unpaired Student's *t* test. **c** RNA-seq analysis of M1 macrophage polarisation markers in orthotopic tumours.

IHC analysis: CD68(ab213363), CD3 (ab52959), CD8 (ab237710), PRF1 (ab75573) from Abcam (Cambridge, UK). Ki67 (D3B5, 9129s) from Cell Signaling Technology (CST, Danvers) was used for both animal and human tissues.

Flow cytometry analysis of tumour-infiltrating immune cells

Flow cytometry-based immune phenotype of tumours was performed according to already published protocols [33]. One million of cells were stained with the appropriate antibodies: T cells, $CD45^+$ $CD3^+$; Macrophages, $CD45^+$, $CD11b^+$, $f4/80^+$; NK cells, $CD45^+$ $CD49b^+$. Antibodies: CD3 (FITC, 100204), CD45 (BV421, 103134), CD86 (PE, 105106) CD11b (PERCP, 101228) from Biolegend (Biolegend, San Diego, California, USA), F4/80 (48-4801-82) from ebioscience (Thermo Fisher Scientific, Waltham, Massachusetts, USA). Samples were acquired on a FACS Canto II (BD Biosciences, San Jose, California, USA) and analysed with FlowJo software (FlowJo LLC, Ashland, Oregon, USA).

RNA-sequencing (RNAseq)

RNA integrity number (RIN) was measured on an Agilent Bio Analyzer 2100 system. Only RNA samples with a RIN > 7 were used for cDNA library construction. All cDNA libraries were sequenced using paired-end strategy (read length 150 bp) on an Illumina HiSeq 2000 platform.

Quality of raw reads was checked with FASTQC. Transcripts were quantified with the alignment-free method implemented in Salmon 0.11.3 [34]. Mouse genome and transcriptome from Genecode Release M18 (GRCm38.p6) were used. Differential expression analysis was performed with NOISeq R package [35]. Gene Set Enrichment analysis of deregulated genes was performed using enrichR package [36].

Statistical analysis

Differences in survival duration were determined using a log-rank test. All statistical tests were two-sided, and a *P* value less than 0.05 indicated statistical significance. All statistical analyses and Kaplan–Meier curves

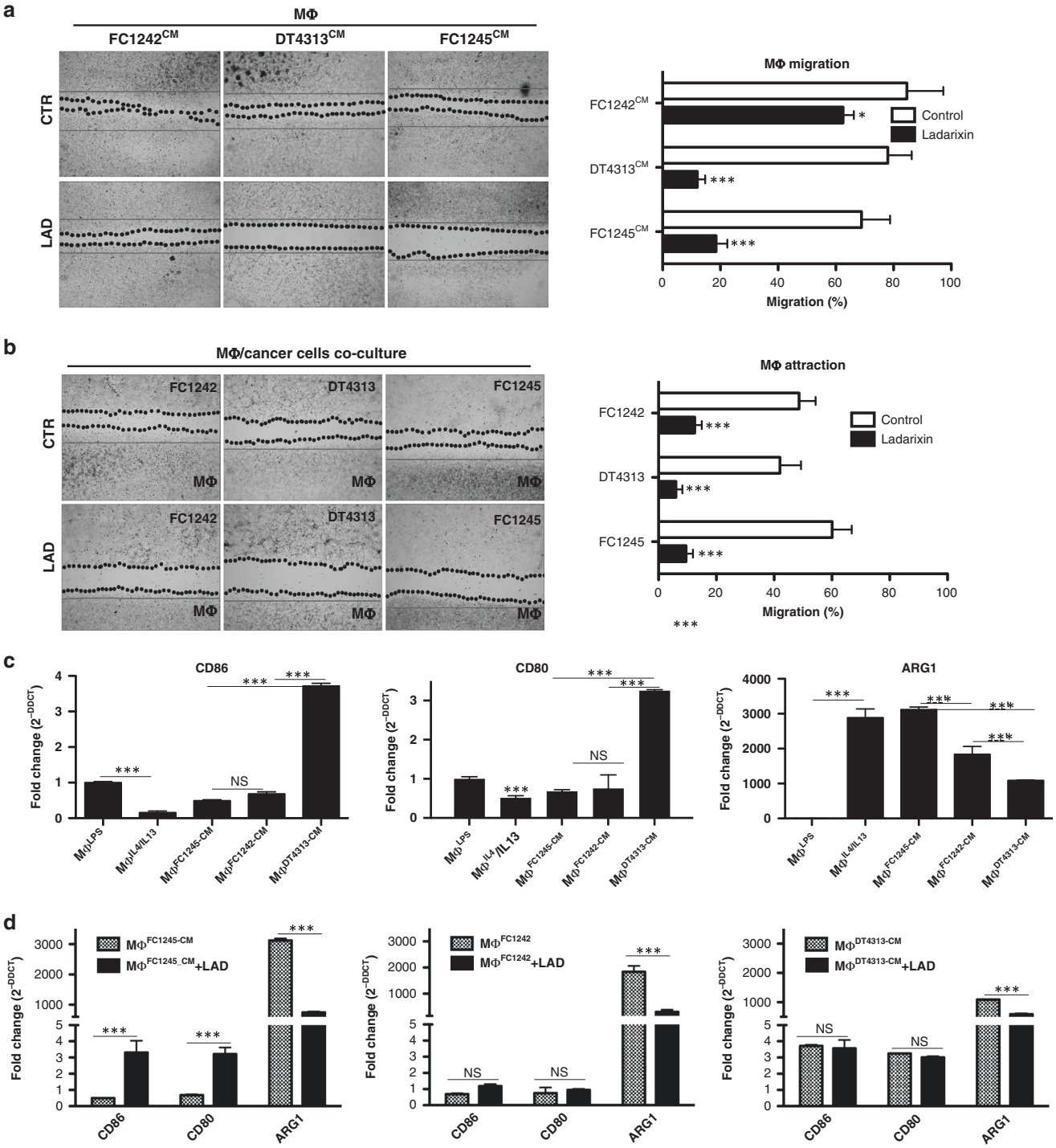

Fig. 2 Effect of Ladarixin on tumour-mediated polarisation and migration of bone marrow-derived macrophages (BMDM). a Wound-healing migration assay of macrophages cultured with conditioned medium from the indicated cancer cells with or without ladarixin treatment after 24 h respect to T0 (red line). Wound healing is expressed as percentage closure (mean and standard error values are shown) relative to original size: [(wound area at 24 h) − (original wound area, T0)/original wound area, T0)] × 100. The mean values and SD are shown. Photographs of the wound area were taken using phase contrast microscopy immediately and 24 h after the incision. **b** Attraction of macrophages co-cultured with the indicated cancer cells with or without ladarixin treatment after 24 h respect to T0 (red line); The mean values and SD are shown. Photographs of the wound area were taken using phase contrast microscopy immediately and 24 h after the incision. **c** Gene expression levels of M1/M2 polarisation markers in macrophages cultured with conditioned medium from the indicated cancer cells. LPS and IL-4/IL-13 treatments are used as control for M1 and M2 polarisation, respectively. qRT-PCR data are expressed as the fold change in RNA expression between the gene of interest and β-actin. Mean and SD are shown. **d** Gene expression levels of M1/M2 polarisation markers in macrophages co-cultured with conditioned medium cancer cells with or without ladarixin treatment (10 mM). The mean values and SD are shown. ***$P < 0.001$, **$P < 0.01$; *$P < 0.05$, by two-tailed unpaired Student's t test.

were performed using GraphPad Prism 5 software (GraphPad Software, San Diego, CA). For differential expression analysis with NOISeq package we filtered out the genes with a log2 fold change <1.5 and a variance difference (Cohen's d) <0.85. For the enrichment analysis, only the pathways with a FDR > 0.05 were considered. Mice sample size estimation was based on our previous papers [24, 26, 37].

RESULTS

PDAC CDG mouse models recapitulate the human transcriptomic and immunological features

To evaluate the potential therapeutic effects of CXCR1/2 inhibition in different PDAC subtypes, we took advantage of our previously described in vivo cancer models which resemble human PDAC subtypes and display high-, low- and no- immunogenic potential based on the ability of these cells to evoke an immune response when orthotopically implanted in syngeneic recipient mice [24].

CDGs with different immunogenic and molecular features (Fig. 1a) were obtained injecting PDAC-derived cell lines into the pancreas of recipient syngeneic C57BL6/J mice and observed until evidence of tumour bulk formation. Notably, IHC analysis of MicroSatellite Instability (MSI) markers demonstrated that all models were microsatellite stable (data previously published) [24].

By cytofluorimetric analysis, we then characterised each excised tumour for immune features and confirmed that models with best prognosis (DT4313 and DT6606) were also those that retained the ability to evoke a moderate immune response, while models with worst prognosis (FC1245 and CR705) displayed no-immunogenic potential. In particular, these latter more-aggressive models displayed a lower percentage of T and NK cells with respect to the others (Fig. 1b). Moreover, bulk RNA-seq analysis of both orthotopic (Fig. 1c) and subcutaneous (Supplementary Fig. 1) tumours with high-, low- and no-immunological potential showed a marked increase of markers of M1 macrophages polarisation (Stat1, Nos2, Socs3, Cxcl9, Cxcl10, Cxcl11, IFNγ) in high-immunological potential CDGs compared to the others.

Altogether these data demonstrated that high percentage of M1 TAMs and the existence of a high-immunogenic potential are strictly correlated with a better prognosis in our models.

In vitro characterisation of Ladarixin effects

Ladarixin affects tumour-mediated M2 polarisation and migration of bone marrow-derived macrophages (BMDM). We have recently demonstrated that pancreatic neoplastic progression is associated with an increased accumulation of macrophages [37]. Thus, we investigated whether tumour-secreted factors in conditioned medium from our models (Fig. 2a), as well as the direct co-culture of BMDM and PDAC cells (Fig. 2b), can affect macrophage migration, and tested the potential effects of ladarixin treatment in these contexts. In both cases, we observed that macrophages had similar migration and attraction rates when stimulated with conditioned medium from CDG cells with different immunological potential or co-cultured with them, and notably, CXCR1/2 inhibition by ladarixin reverted these effects (Fig. 2a).

As no significant differences were observed in the ability of different CDG cell types to induce the migration of macrophages or to attract them, we then tested the capability of CDG-secreted factors to influence M1/M2 macrophage polarisation. C57BL6 BMDM were thus cultured with conditioned medium from CDG cell lines using LPS and IL-4/IL-13 as positive controls of M1 and M2 polarisation, respectively. Real-Time qPCR analysis showed that conditioned medium from high-immunogenic, less-aggressive DT4313 model clearly induced a macrophage switch toward an anti-tumour M1 phenotype (high CD86 and CD80, low ARG1), while conditioned medium from low- or no-immunogenic, more-aggressive FC1242 and FC1245 models directed the switch toward an M2 phenotype (Fig. 2c). Treatment with ladarixin was able to revert this M2 macrophage polarisation, and, notably, in FC1245 ladarixin also significantly induced the expression of both M1 markers CD86 and CD80 (Fig. 2d).

To investigate the possible direct effects of ladarixin on tumour cells, CDG cell lines were treated in vitro with increasing doses of ladarixin for 72 h and analysed for proliferation and migration ability. Although CXCR1 and CXCR2 are expressed also on tumour cells (data not shown), ladarixin treatment did not affect cancer cell proliferation (Fig. 3a) and influenced spontaneous migration of only DT4313 (Fig. 3b). To investigate possible effects of a CXCR1/2 agonist on CXCR1/2 expression on tumour cells, CDG cell lines were treated in vitro with IL-6 (100 ng/mL) and analysed for expression at specific timepoints. Although CXCR1 and 2 are poorly expressed in cancer cells (difference in expression with b-actin of about 20 cycles DCT = 17–20), IL-6 slightly affected their expression (Supplementary Fig. 2).

In vivo characterisation of Ladarixin effects in PDAC models

Ladarixin induces tumour shrinkage in CDG PDAC mouse models promoting a suppressive to permissive immune transition and increasing anti-PD-1 treatment efficacy. To evaluate whether CXCR1/2 inhibition by ladarixin could reduce tumour growth and ameliorate the immune state of PDAC models with different immunogenic potential, C57BL/6J mice were subcutaneously injected with DT4313 and FC1245 CDG ($n = 8$ for each cell line) and randomly assigned to receive ladarixin (15 mg/Kg, i.p. daily for three weeks) or vehicle, as control, and anti-PD-1 (6 mg/Kg or IgG, i.p. twice a week for two weeks) alone or in combination with ladarixin. Treatment with anti-PD-1 was started one week after

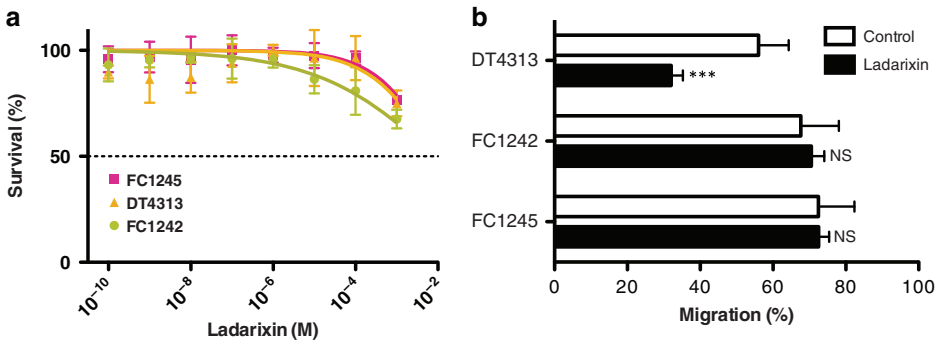

Fig. 3 Ladarixin in vitro effect on tumour cells. a Effects of ladarixin on tumour cell proliferation. Percent relative proliferation of the indicated cancer cells 72 h after treatment with increasing concentrations of ladarixin are shown. Vehicle-treated cells were assigned a value of 100% and designated as control. Means and 95% CIs are shown. **b** Wound-healing migration assay of cancer cell models untreated or treated with ladarixin for 48 h. Wound healing is expressed as a percentage of wound-healing closure (mean and standard error values are shown) relative to original size. Photographs of the wound area were taken using phase contrast microscopy immediately and 48 h after the incision. Mean and SD are shown. ***$P < 0.001$, NS not significant, by two-tailed unpaired Student's t test.

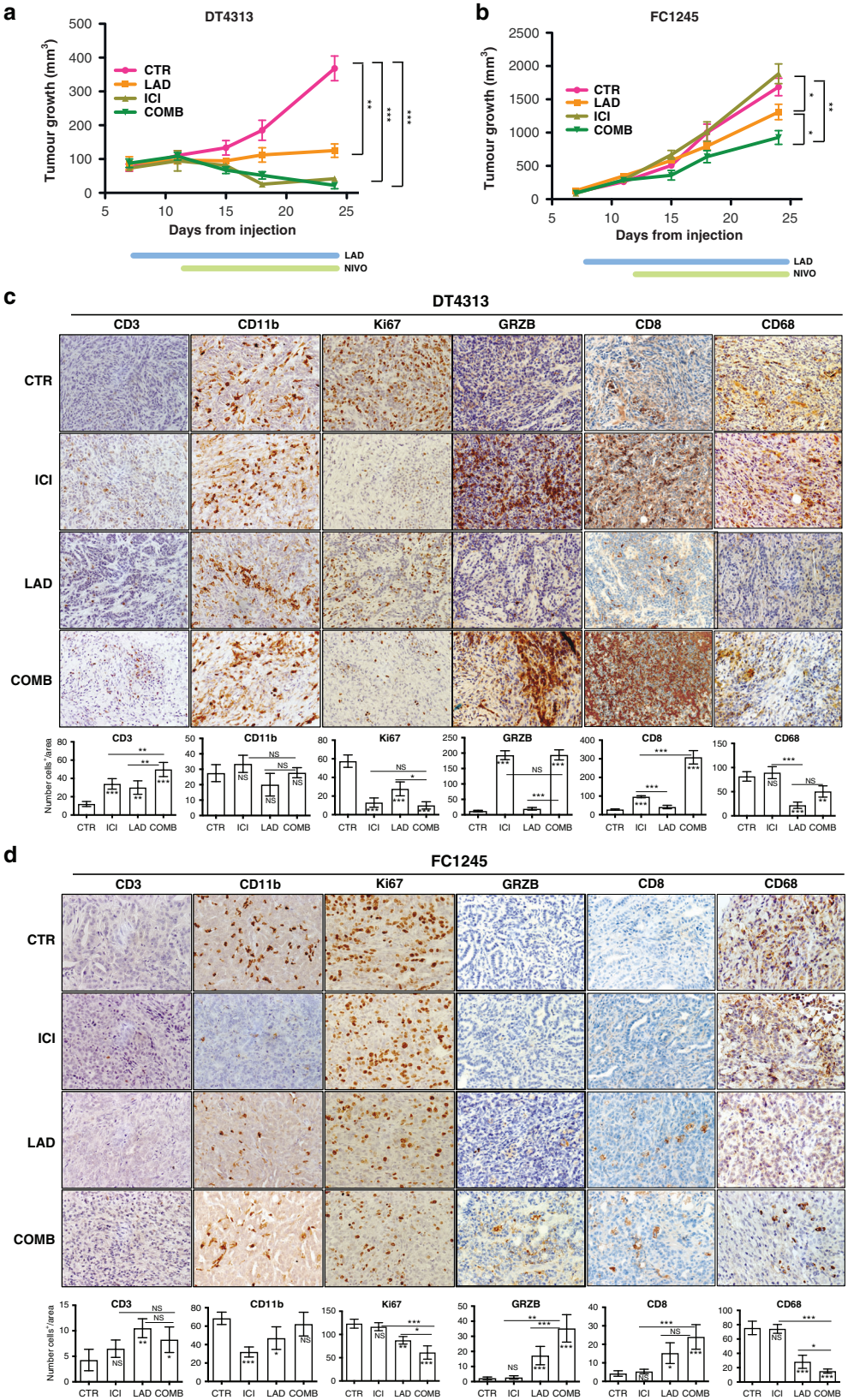

Fig. 4 Pancreatic cancer CDG mouse models. C57BL6/J mice bearing DT4313 (**a**) and FC1245 (**b**) CDGs were randomly assigned to four groups to receive ladarixin (15 mg/Kg, i.p. daily) or vehicle, as control, and anti-PD-1 (6 mg/Kg or IgG, i.p. twice a week for 2 weeks) alone or in combination with ladarixin; differences among survival duration of mice in each group were determined by log-rank test; Mean and SEM are shown (***$P < 0.001$, **$P < 0.005$; *$P < 0.05$). **c**, **d** Upper panels: immunohistochemical analysis of CDGs excised tissues; lower panels of figure, quantification analysis of each marker is provided as the average number of positive cells per mm^2. From 4–8, individual areas per case were examined. Statistical differences were calculated by Student's *t* test. *$P < 0.05$; **$P < 0.01$; ***$P < 0.001$.

ladarixin administration. As expected, anti-PD-1 treatment showed a great efficacy in inducing the shrinkage of DT4313 high-immunological potential tumours, but, quite surprisingly, also ladarixin as single agent significantly reduced tumour growth of this CDG model (ctr vs lad, $P = 0.001$; ctr vs comb, $P < 0.001$; lad vs comb, $P = 0.004$; ctr vs anti-PD-1, $P = 0.001$) (Fig. 4a).

In non-immunogenic FC1245 model on the contrary, anti-PD-1 treatment had no effect on tumour volume, while ladarixin alone and, more efficiently, the combination treatment of ladarixin with the anti-PD-1 significantly increased tumour volume shrinkage (ctr vs lad, $P = 0.049$; ctr vs comb, $P = 0.003$; lad vs comb, $P = 0.043$; anti-PD-1 vs comb, $P = 0.001$) (Fig. 4b).

To study the mechanisms underlying ladarixin effects on tumour growth, immune cell infiltration analysis by IHC was performed in the different CDG models. At baseline, DT4313 model was characterised by a significant inflammatory immune infiltration into the tumour bulk. Ladarixin treatment increased the number of $CD8^+$ tumour-infiltrating lymphocytes (TILs), while only slightly increased the percentage of $CD11b^+$ cells as well as of $GRZB^+$ cytotoxic effector cells and decreased $CD68^+$ macrophages. On the contrary, anti-PD-1 as single agent increased the percentage of TILs as well as of GRZB expression and decreased $Ki67^+$ cells, while the combination further increased the percentage of CD11b+ and TILs compared to anti-PD-1 treatment alone and reduced $CD68^+$ cells, indicating the positive contribution of ladarixin to anti-PD-1 efficacy (Fig. 4c). Untreated non-immunogenic FC1245 model showed only a modest infiltration of T cells (Fig. 4d), and ICI as single agent did not have any effect on the percentage of $Ki67^+$ and $CD68^+$ cells, TILs and GRZB expression. Ladarixin alone instead increased the percentage of TILs and also slightly increased the percentage of

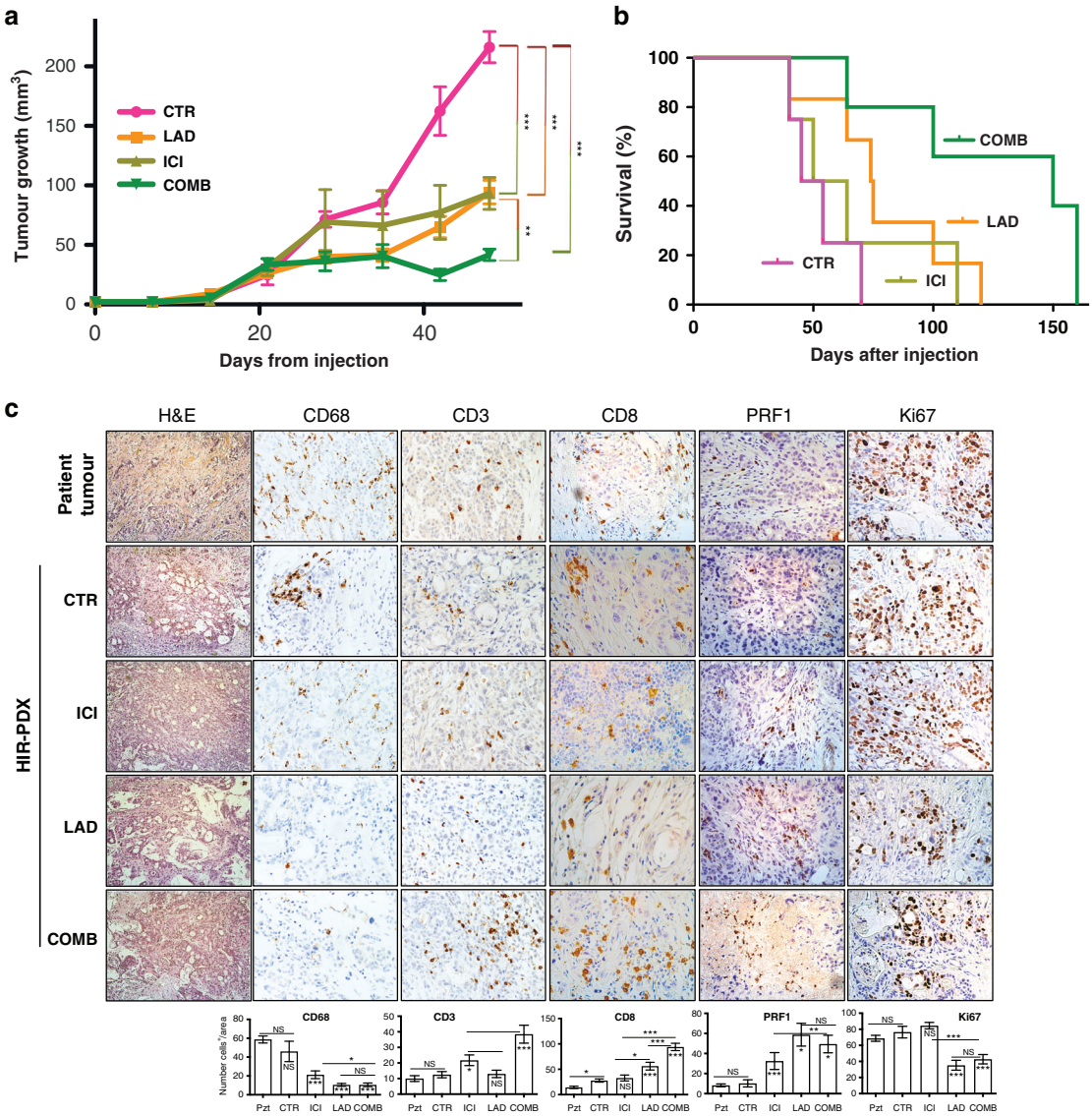

Fig. 5 Orthotopic patient-derived xenograft (PDX) in human immune-reconstituted (HIR) mice. a hu-CD34+ mice were orthotopically injected with PDAC patient-derived cancer tissue. HIR-PDX mice were randomly assigned to receive vehicle, ladarixin (15 mg/Kg, i.p. daily), and Nivolumab (ICI, 6 mg/Kg or IgG, i.p. twice a week for 2 weeks) alone or in combination with ladarixin (15 mg/Kg daily). CTR vs LAD, *P* value: 0.0077; CTR vs ICI, *P* value: 0.0041; CTR vs COMB, *P* value: 0.0098; LAD vs COMB, *P* value: 0.0020; ICI vs COMB, *P* value: 0.0362. **b** Kaplan–Meier survival analysis of PDX-HIR mice. Mice were sacrificed by carbon dioxide inhalation when evidence of advanced bulky disease developed. The day of sacrifice was considered the day of death from disease for the purpose of survival evaluation. Differences among survival duration of mice in each group were determined by log-rank test. **c** Immunohistochemical analysis of excised tumours. Quantification analysis of each marker is provided as the average number of positive ells per mm^2. From 4–8, individual areas per case were examined. Statistical difference was calculated by Student's *t* test. $^*P < 0.05$; $^{**}P < 0.01$; $^{***}P < 0.001$.

CD11b+ cells and GRZB expression, while reduced the percentage of Ki67$^+$ cells. Finally, the combination treatment strikingly reduced Ki67$^+$ and CD68$^+$ cells and increased the number of TILs and GRZB expression (Fig. 4d).

These results demonstrated that, regardless of the immunogenic potential, ladarixin promotes the entry of cytotoxic T cells into the tumour, ultimately acting synergistically with anti-PD-1 to increase tumour shrinkage. However, the subsequent recognition of tumour cells by TIL is strictly dependent by intrinsic characteristic of cancer cells, thus resulting in a more moderate response in CDG with no-immunogenic potential respect to high-immunogenic potential ones.

Combination of ladarixin plus ICI (nivolumab) reduces tumour growth and increases survival of HIR-PDX mice. We established a patient-derived xenograft (PDX) model by implanting in BALB/c nude mice a human PDAC tumour of the immunological subtype, according to Bailey classification. After tissue expansion, fractioned PDX pieces were orthotopically injected in human immune-reconstituted (HIR) mouse models ($n = 20$) (hu-CD34+ NSG mice). We matched PDAC patient and CD34 donor according to HLA-DR allele to generate hu-CD34+ NSG tumour-bearing mice. Peripheral blood samples from each HIR mouse were checked for immune cell components along with recipient BALB/c nude mouse before the orthotopic injection (Supplementary

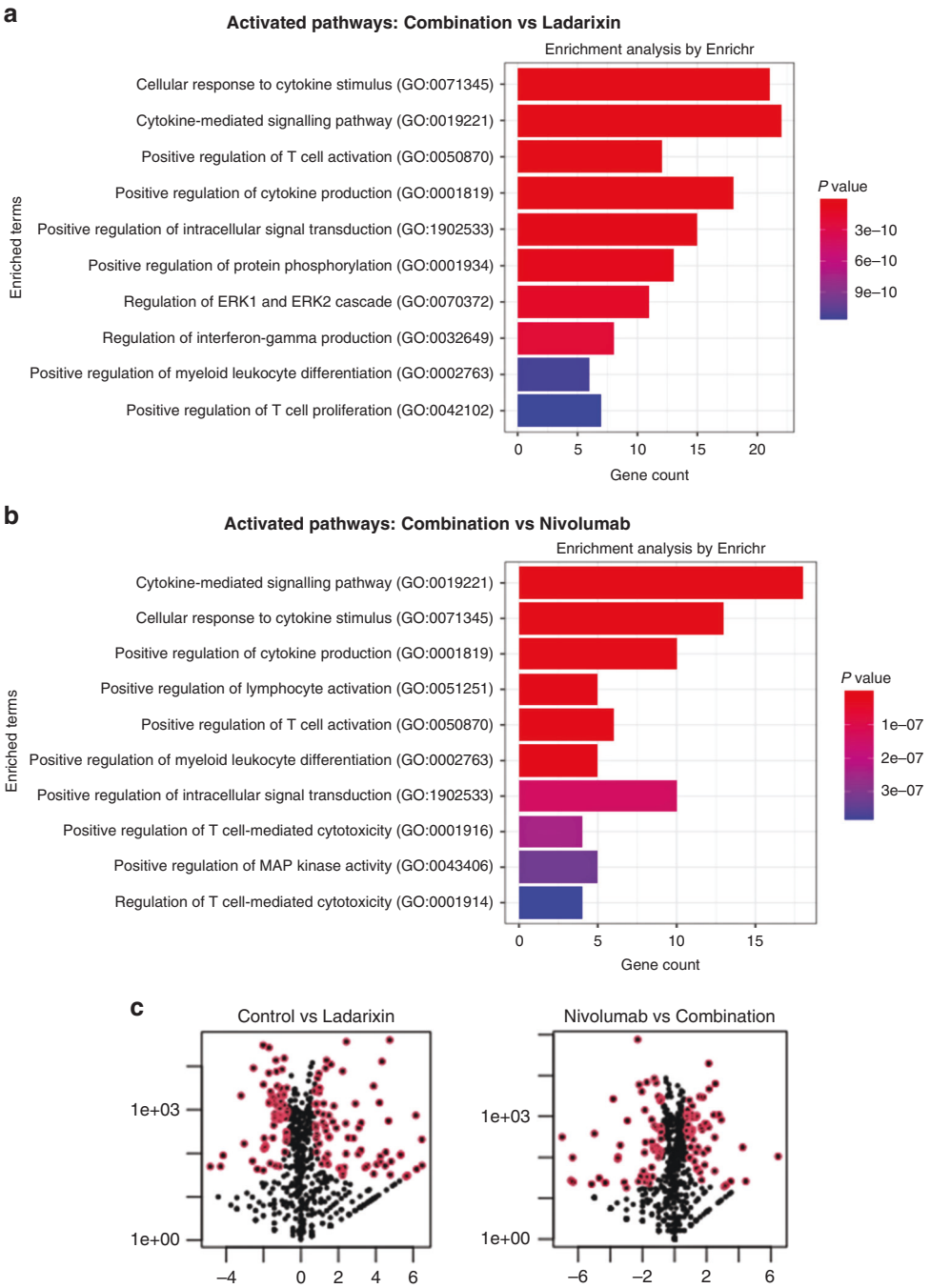

Fig. 6 Gene ontology (GO) biological processes analysis in the combination treatment versus single treatment. Enrichment analysis showing top ten activated pathways in tumours treated with the combination compared to Ladarixin (**a**) and Nivolumab (**b**). **c** The relevant volcano plots of the top ten activated pathways in tumours treated with combination compared to Ladarixin and Nivolumab.

Tables 1 and 2). In order to prevent issues due to the development of incorrect percentage ratio of the immune subpopulation, we monitored the percentage of human and mouse B (CD19+) and T (CD3+) cells over the time and randomised mice in each treatment group according to their immune-system status to prevent group variability. HIR-PDX mice were randomly assigned to receive vehicle, ladarixin (15 mg/Kg daily), and Nivolumab (6 mg/Kg or IgG, i.p. twice a week for two weeks) alone or in combination with ladarixin as in Fig. 4a, b.

In HIR-PDX mice, nivolumab treatment showed a great efficacy in inducing volume shrinkage of high-immunogenic potential human tumour (Fig. 5a), and in line with data obtained in CDG PDAC mouse models, also ladarixin as a single agent showed a reduction of tumour volume near to that obtained with ICI treatment (Fig. 5a). Notably, the combination of ladarixin with nivolumab led to a statistically significant reduction of tumour volume compared to nivolumab or ladarixin alone (Fig. 5a).

The effect of Ladarixin, nivolumab and combination treatment on median survival rate was also examined (Fig. 5b). We found that nivolumab treatment failed to prolong HIR-PDX mouse median survival (49.5 days vs 57 days; $P = 0.549$), while ladarixin as single agent slightly increased median survival (49.5 days vs 74.5 days; $P = 0.044$). Once again, the combination treatment was more effective than both treatments alone and significantly extended mouse median survival (49.5 days vs 150 days, $P = 0.0108$) (Fig. 5b).

To analyse the effects of ladarixin on immune TME, we initially evaluated the retention of morphopathological and immune infiltrate characteristics of HIR-PDX model, comparing this model with tumour specimen from patients (Fig. 5d, upper side). Analysing the effects of the different treatments on the HIR-PDX model of PDAC, we then found that anti-PD-1 as single agent induced only an increase of perforin 1 expression and a reduction of CD68 positive cells compared to vehicle, while it did not change the percentage of $Ki67^+$ tumour cells and CD8 infiltration. On the other hand, ladarixin alone reduced $Ki67^+$ tumour cells and the number of $CD68^+$ macrophages infiltrating the tumour and increased the percentage of TILs and perforin 1 into the tumour. Finally, combination treatment reduced the percentage of $Ki67^+$ tumour cells and the number of $CD68^+$ macrophages infiltrating the tumour, while it dramatically increased the number of TILs and perforin 1 release (Fig. 5c).

Having assessed the effects of the treatments on immune TME, we then analysed the effect of ladarixin and combination treatment on tumours by RNA-sequencing and Gene Ontology (GO) analysis (Fig. 6). As expected, nivolumab mainly up-regulated genes involved in inflammatory response with induction of T cells proliferation, while ladarixin modulated genes involved in a type of immune response driven by interferon (Supplementary Fig. 3). More importantly, gene enrichment analysis showed an increase in T cells proliferation, activation and cytotoxicity, and positive regulation of myeloid leucocyte differentiation in the combination treatment compared to nivolumab and ladarixin alone (Fig. 6). Thus, the addition of ladarixin to nivolumab treatment is able to reduce tumour growth and increase immune cells activation amplifying the effect of single agents.

DISCUSSION

No effective pharmacological approach is currently available for the treatment of aggressive PDAC [7, 38]. Receptors CXCR1/2 have proved to be crucially involved in tumour progression, treatment resistance and metastasis [39]. In line with this, inhibitors of CXCR1/2, including small molecules or specific antibodies, showed great efficacy in treating tumours, such as cutaneous and uveal melanomas, where the inhibition of CXCR1/2 and their ligands (CXCL1/2/3/7/8) yielded promising results [40].

In this study, we demonstrate that ladarixin, a potent CXCR1-2 inhibitor, can effectively block macrophage attraction and M2 polarisation, and thus trigger an immunosuppressive to immunopermissive transition in PDAC mouse and human models, providing the rational for its use in combination with an immunocheckpoint inhibitor, especially for the treatment of non-immunogenic, highly aggressive PDAC subtype.

We initially evaluated the ability of pancreatic cancer models with different immunogenic features (high-, low- and no-immunogenic potential) to evoke an immune response and to attract macrophages. Analysing the gene expression, we found that M1 polarisation marker expression was strongly correlated with the immunogenic potential of our cancer models and with a better prognosis, while a predominant M2 marker expression was observed in models with no or low immunogenic potential which also presented a worse prognosis. In vitro, CDG pancreatic cancer models comparably induced macrophages mobilisation (if cultured with conditioned medium of each CDG model) or attraction (if co-cultured with each CDG model). However, cells with no or low immunogenic potential (FC1242 and FC1245) strongly directed the polarisation of macrophages towards the M2 immunosuppressive type, while high-immunological potential DT4313 CDG model showed increased gene expression of CD80 and CD86 M1 markers and a reduction of ARG1 M2 marker. In this setting, ladarixin as a single agent was surprisingly able to reduce the attraction and migration of macrophages, as well as to impair M2 polarisation induced by tumours, and in particular that induced by those with no or low immunogenic potential. As IL-8 is known to selectively attract neutrophils [41] while having little or no effect on monocytes [42], these effects were quite unexpected and can be explained considering the potential involvement of other chemokines and cytokines of the TME, which might act synergistically in regulating the recruitment of mononuclear cells [43]. Studies have demonstrated in fact that IL-8-mediated chemotaxis can be induced in monocytes following exposure to two cytokines, IL-4 and IL-13, which are produced by multiple components in the TME of pancreatic cancer [44] and were shown to induce the up-regulation of CXCR1 and CXCR2 expression in macrophages, thus triggering a biological programme that reorients the action of IL-8 to monocytes and contributes to the formation of the mononuclear phagocyte infiltrate [42]. Although we have observed only the result of this possible cooperation between cytokines and chemokines, the fact that, on the contrary, ladarixin did not affect cancer cell proliferation and only weakly influenced their migration (despite the expression of CXCR1 and CXCR2 by tumour cells), further indicates the crucial role of the interaction of the other components of the tumour milieu in inducing macrophage to respond to IL-8 (i.e., migration and M1/M2 polarisation). in our cancer models and [45] highlights the remarkable potential impact of IL-8 inhibition for cancer treatment. Driven by the results obtained in vitro, we then evaluated the effects of ladarixin in vivo in our CDG models with high- and no- immunogenic potential. While effectively inducing tumour shrinkage in the syngeneic high-immunogenic model (DT4313) [24], the anti-PD-1 treatment had no effect on tumour growth in syngeneic tumour model with no-immunogenic potential (FC1245), where, however, ladarixin as single agent showed slight efficacy, and the combination treatment with ladarixin and anti-PD-1 significantly reduced tumour volume, displaying an appreciable efficacy in this aggressive PDAC subtype [24, 38, 46, 47].

The impairment of macrophage attraction and M2 polarisation obtained with ladarixin treatment was thus instrumental to increase the susceptibility of tumour to the immune system, which could be then further helped by the inhibition of immune checkpoints (anti-PD-1 treatment). These results are of particular significance because obtained with FC1245 CDG cells, which constitute a very aggressive PDAC model because of its capacity to escape from the immune system [24] further support previous data showing that systemic ladarixin treatment of melanoma-

bearing mice polarised intratumoral macrophages to M1 phenotype, abrogated intratumoral de novo angiogenesis and inhibited melanoma self-renewal [40]. In addition to the effects mediated by the macrophages, we can also hypothesise that the tumour shrinkage that we observed following ladarixin treatment could also be due to other effects of the compound on the immune system, as for example [48] the inhibition of CXCR2-mediated biological aging of neutrophils, which has been recently shown to effectively compromise the progression of malignancies and has been proposed as a potential new strategy for the treatment of oncological disorders [49].

In order to improve the relevance of our data to the human disease and accelerate the clinical translation of our findings, we then used human immune-reconstituted (HIR) mouse models, a forefront preclinical model to support studies on immune-based therapies. Unlike patient-derived xenograft (PDX) model obtained engrafting human tumours in immune-deficient mice that reproduce main feature of human host tumour, but fail to recapitulate immune context [50], and syngeneic tumour mouse models that not fully reproduce all human-specific pathways and lack the direct connection with personalised medicine, HIR models provide in fact a relevant in vivo context to understand human-specific tumour-immune interaction as they combine human immune-system repopulation with PDX models [51]. This feature is particularly important when studying the biology of the IL-8 pathway as several differences exist between the human and the murine IL-8/CXCR axis [18, 52]. As expected, the human immunogenic subtype of PDAC had almost the same response of the high-immunogenic potential syngeneic cancer model to ICI and ladarixin as single agents and in combination. As in the corresponding syngeneic models, ladarixin reduced the macrophage population into the tumour, and increased M1 macrophage polarisation, ultimately hampering tumour growth in HIR mice, thus confirming the induction of an immunopermissive TME by ladarixin and demonstrating the efficacy of a combined CXCR1/2 inhibitor and anti-PD-1 treatment in a mouse model bearing human immune system and orthotopically injected with a patient-derived PDAC immunogenic subtype. These results confirm recently published ones [16], but adding, notably, the novel aspect of the effects of CXCR1/2 inhibition on macrophage infiltration and polarisation in the tumour, and how these phenomena affect PDAC pathogenesis.

In conclusion, previous studies have discussed and prospected the use of novel immunoadjuvants for pancreatic cancer treatment [53, 54] but no evidence on immune-system activation by ICI in low or no-immunogenic subtypes of PDAC has been provided so far. Here, we discovered the ability of ladarixin to convert a pro-tumoral into an immunopermissive microenvironment by also, unexpectedly, affecting infiltration and polarisation of macrophages in the TME, thus highlighting the effects of IL-8/CXCR1-2 axis inhibition on TAMs and, especially, how these effects might potentially affect PDAC pathology and treatment. Using both syngeneic and HIR mouse models, we in fact demonstrated, for the first time, that ladarixin and ICI combination has synergistic anti-tumoral effects and can be an effective approach for the treatment of PDAC, especially significant when treating PDAC subtypes that are usually refractory to immunotherapy.

DATA AVAILABILITY

The data of this study are available from the corresponding author upon request.

REFERENCES

1. Siegel RL, Miller KD, Fuchs HE, Jemal A. Cancer statistics, 2021. CA Cancer J Clin. 2021;71:7–33.
2. Royal RE, Levy C, Turner K, Mathur A, Hughes M, Kammula US, et al. Phase 2 trial of single agent ipilimumab (Anti-CTLA-4) for locally advanced or metastatic pancreatic adenocarcinoma. J Immunother. 2010;33:828–33.
3. Brahmer JR, Tykodi SS, Chow LQM, Hwu WJ, Topalian SL, Hwu P, et al. Safety and activity of anti–PD-L1 antibody in patients with advanced cancer. N. Engl J Med. 2012;366:2455–65.
4. O'Reilly EM, Oh DY, Dhani N, Renouf DJ, Lee MA, Sun W, et al. Durvalumab with or without tremelimumab for patients with metastatic pancreatic ductal adenocarcinoma. JAMA Oncol. 2019;5:1431.
5. Karamitopoulou E. Tumour microenvironment of pancreatic cancer: immune landscape is dictated by molecular and histopathological features. Br J Cancer. 2019;121:5–14.
6. Li R, He Y, Zhang H, Wang J, Liu X, Liu H, et al. Identification and validation of immune molecular subtypes in pancreatic ductal adenocarcinoma: implications for prognosis and immunotherapy. Front Immunol. 2021;12:2829.
7. Liu X, Xu J, Zhang B, Liu J, Liang C, Meng Q, et al. The reciprocal regulation between host tissue and immune cells in pancreatic ductal adenocarcinoma: new insights and therapeutic implications. Mol Cancer. 2019;18:184.
8. Yan S, Wan G. Tumor-associated macrophages in immunotherapy. FEBS J. 2021;288:6174–86.
9. Powell D, Lou M, Barros Becker F, Huttenlocher A. Cxcr1 mediates recruitment of neutrophils and supports proliferation of tumor-initiating astrocytes in vivo. Sci Rep. 2018;8:13285.
10. Alfaro C, Teijeira A, Oñate C, Pérez G, Sanmamed MF, Andueza MP, et al. Tumor-produced interleukin-8 attracts human myeloid-derived suppressor cells and elicits extrusion of neutrophil extracellular traps (NETs). Clin Cancer Res. 2016;22:3924–36.
11. Highfill SL, Cui Y, Giles AJ, Smith JP, Zhang H, Morse E, et al. Disruption of CXCR2-mediated MDSC tumor trafficking enhances anti-PD1 efficacy. Sci Transl Med. 2014;6:237ra67.
12. Bakouny Z, Choueiri TK. IL-8 and cancer prognosis on immunotherapy. Nat Med. 2020;26:650–1.
13. Wu L, Xie S, Wang L, Li J, Han L, Qin B, et al. The ratio of IP10 to IL-8 in plasma reflects and predicts the response of patients with lung cancer to anti-PD-1 immunotherapy combined with chemotherapy. Front Immunol. 2021;12:1113.
14. Schalper KA, Carleton M, Zhou M, Chen T, Feng Y, Huang SP, et al. Elevated serum interleukin-8 is associated with enhanced intratumor neutrophils and reduced clinical benefit of immune-checkpoint inhibitors. Nat Med. 2020;26:688–92.
15. Yuen KC, Liu LF, Gupta V, Madireddi S, Keerthivasan S, Li C, et al. High systemic and tumor-associated IL-8 correlates with reduced clinical benefit of PD-L1 blockade. Nat Med. 2020;26:693–8.
16. Li P, Rozich N, Wang J, Wang J, Xu Y, Herbst B, et al. Anti-IL-8 antibody activates myeloid cells and potentiates the anti-tumor activity of anti-PD-1 antibody in the humanized pancreatic cancer murine model. Cancer Lett. 2022;539:215722.
17. Chao T, Furth EE, Vonderheide RH. CXCR2-dependent accumulation of tumor-associated neutrophils regulates T-cell immunity in pancreatic ductal adenocarcinoma. Cancer Immunol Res. 2016;4:968–82.
18. Teijeira A, Garasa S, Ochoa MC, Villalba M, Olivera I, Cirella A, et al. IL8, neutrophils, and NETs in a collusion against cancer immunity and immunotherapy. Clin Cancer Res. 2021;27:2383–93.
19. Horowitz NB, Mohammad I, Moreno-Nieves UY, Koliesnik I, Tran Q, Sunwoo JB. Humanized mouse models for the advancement of innate lymphoid cell-based cancer immunotherapies. Front Immunol. 2021;12:977.
20. de La Rochere P, Guil-Luna S, Decaudin D, Azar G, Sidhu SS, Piaggio E. Humanized mice for the study of immuno-oncology. Trends Immunol. 2018;39:748–63.
21. Shultz LD, Ishikawa F, Greiner DL. Humanized mice in translational biomedical research. Nat Rev Immunol. 2007;7:118–30.
22. Ireland L, Santos A, Ahmed MS, Rainer C, Nielsen SR, Quaranta V, et al. Chemoresistance in pancreatic cancer is driven by stroma-derived insulin-like growth factors. Cancer Res. 2016;76:6851–63.
23. Somerville TDD, Xu Y, Miyabayashi K, Tiriac H, Cleary CR, Maia-Silva D, et al. TP63-mediated enhancer reprogramming drives the squamous subtype of pancreatic ductal adenocarcinoma. Cell Rep. 2018;25:1741–55.e7.
24. Carbone C, Piro G, Agostini A, Delfino P, de Sanctis F, Nasca V, et al. Intratumoral injection of TLR9 agonist promotes an immunopermissive microenvironment transition and causes cooperative antitumor activity in combination with anti-PD1 in pancreatic cancer. J Immunother Cancer. 2021;9:e002876.
25. di Mitri D, Mirenda M, Vasilevska J, Calcinotto A, Delaleu N, Revandkar A, et al. Re-education of tumor-associated macrophages by CXCR2 blockade drives senescence and tumor inhibition in advanced prostate cancer. Cell Rep. 2019;28:2156–68.e5.
26. Santoro R, Zanotto M, Simionato F, Zecchetto C, Merz V, Cavallini C, et al. Modulating TAK1 expression inhibits YAP and TAZ oncogenic functions in pancreatic cancer. Mol Cancer Ther. 2020;19:247–57.
27. Santoro R, Zanotto M, Carbone C, Piro G, Tortora G, Melisi D. MEKK3 sustains EMT and stemness in pancreatic cancer by regulating YAP and TAZ transcriptional activity. Anticancer Res. 2018;38:1937–46.

28. Bertini R, Barcelos LS, Beccari AR, Cavalieri B, Moriconi A, Bizzarri C, et al. Receptor binding mode and pharmacological characterization of a potent and selective dual CXCR1/CXCR2 non-competitive allosteric inhibitor. Br J Pharm. 2012;165:436–54.
29. Garau A, Bertini R, Mosca M, Bizzarri C, Anacardio R, Triulzi S, et al. Development of a systemically-active dual CXCR1/CXCR2 allosteric inhibitor and its efficacy in a model of transient cerebral ischemia in the rat. Eur Cytokine Netw. 2006;17:35–41.
30. Percie du Sert N, Hurst V, Ahluwalia A, Alam S, Avey MT, Baker M, et al. The ARRIVE guidelines 2.0: updated guidelines for reporting animal research. BMJ Open Sci. 2020;4:e100115.
31. Bailey P, Chang DK, Nones K, Johns AL, Patch AM, Gingras MC, et al. Genomic analyses identify molecular subtypes of pancreatic cancer. Nature. 2016;531:47–52.
32. Zachary AA, Leffell MS. HLA mismatching strategies for solid organ transplantation—a balancing act. Front Immunol. 2016;7:575.
33. Facciabene A, de Sanctis F, Pierini S, Reis ES, Balint K, Facciponte J, et al. Local endothelial complement activation reverses endothelial quiescence, enabling T-cell homing, and tumor control during T-cell immunotherapy. Oncoimmunology. 2017;6:e1326442.
34. Patro R, Duggal G, Love MI, Irizarry RA, Kingsford C. Salmon provides fast and bias-aware quantification of transcript expression. Nat Methods. 2017;14:417–9.
35. Tarazona S, Furió-Tarí P, Turrà D, di Pietro A, Nueda MJ, Ferrer A, et al. Data quality aware analysis of differential expression in RNA-seq with NOISeq R/Bioc package. Nucleic Acids Res. 2015;43:e140.
36. Kuleshov MV, Jones MR, Rouillard AD, Fernandez NF, Duan Q, Wang Z, et al. Enrichr: a comprehensive gene set enrichment analysis web server 2016 update. Nucleic Acids Res. 2016;44:W90–7.
37. Filippini D, Agosto SD, Delfino P, Simbolo M, Piro G, Rusev B, et al. Immunoevolution of mouse pancreatic organoid isografts from preinvasive to metastatic disease. Sci Rep. 2019;9:12286.
38. Yamamoto K, Venida A, Yano J, Biancur DE, Kakiuchi M, Gupta S, et al. Autophagy promotes immune evasion of pancreatic cancer by degrading MHC-I. Nature. 2020;581:100–5.
39. Liu Q, Li A, Tian Y, Wu JD, Liu Y, Li T, et al. The CXCL8-CXCR1/2 pathways in cancer. Cytokine Growth Factor Rev. 2016;31:61–71.
40. Kemp DM, Pidich A, Larijani M, Jonas R, Lash E, Sato T, et al. Ladarixin, a dual CXCR1/2 inhibitor, attenuates experimental melanomas harboring different molecular defects by affecting malignant cells and tumor microenvironment. Oncotarget. 2017;8:14428–42.
41. van Damme J, van Beeumen J, Opdenakker G, Billiau A. A novel, NH2-terminal sequence-characterized human monokine possessing neutrophil chemotactic, skin-reactive, and granulocytosis-promoting activity. J Exp Med. 1988;167:1364–76.
42. Bonecchi R, Facchetti F, Dusi S, Luini W, Lissandrini D, Simmelink M, et al. Induction of functional IL-8 receptors by IL-4 and IL-13 in human monocytes. J Immunol. 2000;164:3862–9.
43. Gouwy M, Struyf S, Noppen S, Schutyser E, Springael JY, Parmentier M, et al. Synergy between coproduced CC and CXC chemokines in monocyte chemotaxis through receptor-mediated events. Mol Pharm. 2008;74:485–95.
44. Shi J, Song X, Traub B, Luxenhofer M, Kornmann M. Involvement of IL-4, IL-13 and their receptors in pancreatic cancer. Int J Mol Sci. 2021;22:2998.
45. Alfaro C, Teijeira A, Oñate C, Pérez G, Sanmamed MF, Andueza MP, et al. Tumor-produced interleukin-8 attracts human myeloid-derived suppressor cells and elicits extrusion of neutrophil extracellular traps (NETs). Clin Cancer Res. 2016;22:3924–36.
46. Foucher ED, Ghigo C, Chouaib S, Galon J, Iovanna J, Olive D. Pancreatic ductal adenocarcinoma: a strong imbalance of good and bad immunological cops in the tumor microenvironment. Front Immunol. 2018;9:1044.
47. Liu YT, Sun ZJ. Turning cold tumors into hot tumors by improving T-cell infiltration. Theranostics. 2021;11:5365–86.
48. Adrover JM, del Fresno C, Crainiciuc G, Cuartero MI, Casanova-Acebes M, Weiss LA, et al. A neutrophil timer coordinates immune defense and vascular protection. Immunity. 2019;50:390–402.e10.
49. Mittmann LA, Haring F, Schaubächer JB, Hennel R, Smiljanov B, Zuchtriegel G, et al. Uncoupled biological and chronological aging of neutrophils in cancer promotes tumor progression. J Immunother Cancer. 2021;9:e003495.
50. Bhimani J, Ball K, Stebbing J. Patient-derived xenograft models—the future of personalised cancer treatment. Br J Cancer. 2020;122:601–2.
51. Liu WN, Fong SY, Tan WWS, Tan SY, Liu M, Cheng JY, et al. Establishment and characterization of humanized mouse NPC-PDX model for testing immunotherapy. Cancers. 2020;12:1025.
52. Stripecke R, Münz C, Schuringa JJ, Bissig K, Soper B, Meeham T, et al. Innovations, challenges, and minimal information for standardization of humanized mice. EMBO Mol Med. 2020;12:e8662.
53. Li R, He Y, Zhang H, Wang J, Liu X, Liu H, et al. Identification and validation of immune molecular subtypes in pancreatic ductal adenocarcinoma: implications for prognosis and immunotherapy. Front Immunol. 2021;12:2829.
54. Li KY, Yuan JL, Trafton D, Wang JX, Niu N, Yuan CH, et al. Pancreatic ductal adenocarcinoma immune microenvironment and immunotherapy prospects. Chronic Dis Transl Med. 2020;6:6–17.

ACKNOWLEDGEMENTS

We would like to thank the Italian Pancreatic Cancer Community (IPCC, www.i-pcc.org) and "Fondazione Nadia Valsecchi Onlus" for the precious networking in the pancreatic cancer field. We would like to thank the members of the Cen.Ri.S. animal facility Mancuso A, Aquilina M and Caristo ME for their valuable assistance during in vivo experiments.

AUTHOR CONTRIBUTIONS

CC, GP, MDP, MA, AS and GT conceived and designed the study; CC and GP designed and performed the majority of the experiments; VC provided cancer cells; FS, EAC, FDS and SU performed experiments; MM and AG performed IHC analyses; AA performed bioinformatics analyses. CC, GP AA, MDP, RN, MA, AAr, AS, VC and GT wrote the manuscript.

FUNDING

This work was supported by the AIRC IG grant number 26330 to GT; AIRC StartUp Grant No. 18178 to VC; AIRC5x1000 grant number 12182 and grant from Italian Ministry of Health FIMCUP_J38D19000690001 to AS; Ministry of Health (CO 2019-12369662) to GT; My First AIRC Grant "Luigi Bonatti e Anna Maria Bonatti Rocca", grant number 23681 to CC.

COMPETING INTERESTS

MDP, RN, MA and AAr are employees of Dompé Farmaceutici S.p.A. The remaining authors declare no competing interests.

ETHICS APPROVAL AND CONSENT TO PARTICIPATE

In vivo experiments were conducted in accordance with the guidelines of the Institutional OPBA and the Italian Ministry of Health Ethics Committee.

CONSENT TO PUBLISH

The study protocol was approved by the Institutional Board of the University of Verona, Verona, Italy. The study was conducted according to the principles of the Declaration of Helsinki and was performed in compliance with Good Clinical Practice guidelines. Written informed consent was obtained.

ADDITIONAL INFORMATION

Supplementary information The online version contains supplementary material available at https://doi.org/10.1038/s41416-022-02028-6.

Correspondence and requests for materials should be addressed to Giampaolo Tortora.

Reprints and permission information is available at http://www.nature.com/reprints

Publisher's note Springer Nature remains neutral with regard to jurisdictional claims in published maps and institutional affiliations.